Journal of Applied Polymer Science

Furfuryl Alcohol Functionalized Graphene Nanosheets for Synthesis of High Carbon Yield Novolak Composites

Hossein Roghani-Mamaqani,[1] Vahid Haddadi-Asl,[2] Mehrzad Mortezaei,[3] Khezrollah Khezri[4]

[1]Department of Polymer Engineering, Sahand University of Technology, P.O. Box 51335-1996, Tabriz, Iran
[2]Department of Polymer Engineering and Color Technology, Amirkabir University of Technology, Tehran, Iran
[3]Department of Polymer Engineering, Islamic Azad University, South Tehran Branch, Tehran, Iran
[4]School of Chemistry, University College of Science, University of Tehran, Tehran, Iran
Correspondence to: H. Roghani-Mamaqani (E-mail: r.mamaghani@sut.ac.ir)

ABSTRACT: Graphene oxide and furfuryl alcohol modified graphene nanosheets (G-FA) were used to prepare graphene/novolak composites. Effect of graphene compatibilization on the properties of the composites especially carbon yield value is evaluated. Both types of graphene nanosheets were dispersed uniquely in the novolak matrix as proved by X-ray diffraction analysis. However, modification of graphene sheets by furfuryl alcohol results in more improved dispersions. Thermogravimetric analysis confirms the elevated thermal stability of the nanocomposites in comparison with the neat novolak. In addition, G-FA containing composites have higher carbon yield values. A shift in the wave number of characteristic bonds of graphene after oxidation and modification with furfuryl alcohol, O—H, C═O, and C—O bonds, are seen in the Fourier transform infrared spectroscopy spectra. Raman results and scanning electron microscopy images show that graphene nanosheets reduced in size and wrinkled by oxidation and functionalization. Transmission electron microscopy image of the composite with 0.2 wt % of G-FA reveals the presence of nanosheets with curvature. © 2013 Wiley Periodicals, Inc. J. Appl. Polym. Sci. **2014**, *131*, 40273.

KEYWORDS: composites; nanostructured polymers; graphene; resins

Received 25 August 2013; accepted 9 December 2013
DOI: 10.1002/app.40273

INTRODUCTION

Phenolics are the first synthetic and commercially used polymer resins. Phenolic resins are prepared by the reaction of phenol or substituted phenol with an aldehyde, especially formaldehyde, in the presence of an acidic or basic catalyst. Resol and novolak, two main types of phenolic resins, differ in the ratio of phenol and formaldehyde and type of the catalyst. In these systems, phenol, formaldehyde, and furfuryl alcohol are used as the reactants to reach a glassy product.[1,2] In addition to the carbonization reactions, furfuryl alcohol also acts as solvent for novolac resins which make it very useful in improving processing condition especially when the resins are used as binding materials. In such applications, viscosity and binding strength of the system can be controlled by varying the amount of furfuryl alcohol.[3,4]

Phenolics are commonly used as thermal resistant thermoset resins in the area of ablative thermal protection. Their low cost, high tensile strength, dimensional stability, age resistance, and fire retardance characteristics after curing make them very attractive.[5] However, low carbon yield value and poor toughness are two main deficiencies of these resins which confine their usage as matrix of ablation resistant composites or precursor for carbon/carbon composites. Several methods have been used to increase carbon yield value of the phenolic resins in which structural modifiers like boron, molybdenum, and phosphorous compounds and additives have drawn more attention.[6–8] Additives with variety of properties, especially nanofillers, can be more attractive to achieve a phenolic resin with high carbon yield value and toughness.

Polymer composites based on carbon black, carbon nanotubes (CNTs), and layered silicates have been used to improve mechanical, thermal, electrical, gas barrier, and some other properties of polymers.[9–13] After discovery of fullerene and CNT, graphene with its extraordinary physical properties considered as a new subject in the science of nanomaterials.[14] Graphene is composed of sp^2-hybridized carbon atoms arranged in a honeycomb structure. It has deeply been investigated due to its excellent electrical, mechanical, and optical properties.[14–18] However, lower functionality of graphene limits its dispersibility in solvents. Therefore, developing efficient chemical methods to functionalize graphene nanosheets has become one of the most critical issues in the production of graphene composites. By taking the advantages of technologies used for dispersing CNTs,[15]

appropriate dispersion of graphene can be achieved. Therefore, modification of graphene nanosheets by species with covalent linkage or non-covalent interactions have been explored to enhance its dispersibility in various media. Thus, using graphene in polymer systems seriously requires its functionalization. Consequently, dispersability of graphene in various polymer matrices results in creation of a new class of polymer composites.[16]

Review of related researches indicates that there are some reports on the curing of phenolic resins in the presence of CNTs; however, there is not any report on the effect of graphene and its functonalization with furfuryl alcohol on the thermal properties of cured novolak resins and its carbon yield value. Men et al.[19] functionalized multi-walled carbon nanotubes (MWCNTs) by furfuryl alcohol moieties. They carried out this funcitonalization process to improve the tribological properties of poly(furfuryl alcohol) by forming poly(furfuryl alcohol) composite coatings via incorporating surface modified CNTs into the matrix. Yen et al.[20] studied the mechanical behavior of phenolic-based composites reinforced with MWCNTs. They dispersed MWCNTs into two types of networks to fabricate phenolic resin composites. They investigated the effects of MWCNT content on the mechanical properties of the composites. Choi et al.[21] functionalized surface of MWCNTs by attachment of phenol anchored azomethine ylides on the surface. They studied effect of the functionalized CNTs on curing kinetics of diglycidyl ether of 4,4′-bisphenol-epoxy mesogenic resin by nonisothermal differential scanning calorimetry at various heating rates. Liu and Ye[22] studied the effects of modified MWCNTs on the curing behavior and thermal stability of a boron phenolic resin. They modified MWCNTs by nitric acid, 4,4′-Diaminodiphenyl methane and also boric acid. They found that the curing apparent activation energy decreases with increasing the amount of modified MWCNTs. However, there is no obvious change in the orders of curing reactions. Cui et al.[23] developed a simple but effective *in situ* polymerization method to prepare phenolic resin-based composites with pristine or carboxylated MWCNTs. They found that the carboxylated MWCNT-filled composites experiences higher thermal stabilities in comparison with the composites with pristine MWCNT. They attributed this to higher dispersion quality of functionalized nanotubes.

In this study, we established a reaction to attach furfuryl alcohol moieties on the edge of graphene oxide (GO) nanosheets. Subsequently, curing of novolak resin in the presence of modified graphene nanosheets and GO has been carried out. These reactions were mainly accomplished to investigate the effect of graphene modification with furfuryl alcohol on the thermal properties and carbon yield value of the graphene/novolak composites. In addition, effect of graphene nanosheets on the various properties of cured novolak resin has been studied. The attachment of furfuryl alcohol on the edge of GO nanosheets has been achieved by an esterification reaction between the hydroxyl groups of furfuryl alcohol and carboxylic groups of GO. Designation of the samples with various types of their filler are summarized in Table I.

Table I. Designation of the Samples with Various Types and Amount of Their Filler

Sample	Graphene type	Graphene content (wt %)
Novolak	–	0
GON0.1	GO	0.1
GON0.2	GO	0.2
GON0.4	GO	0.4
GFAN0.1	G-FA	0.1
GFAN0.2	G-FA	0.2
GFAN0.4	G-FA	0.4

EXPERIMENTAL

Materials

Graphite was purchased from Merk, Germany. Novolak resin (IP502) was purchased from Resitan Company, Iran. Graphite was purchased from Merk, Germany. Furfuryl Alcohol (Sigma–Aldrich, 98%), hexamethyltetramine (HMTA, Sigma–Aldrich, 99%), N,N′-dicyclohexylcarbodiimide (DCC, Aldrich, 99%), 4-dimethylaminopyridine (DMAP, Aldrich, 99%), sodium nitrate (Sigma–Aldrich, 99%), potassium permanganate (Fluka, 99%), N,N-dimethylformamide (DMF, Sigma, 99%), and sulfuric acid (Merck) were used as received.

Preparation of GO

GO was prepared using modified Hummers' method. 1.5 g $NaNO_3$ and 3.0 g graphite powder were poured into a 300-mL three-necked flask which was placed in an oil bath. Then, 180 mL of H_2SO_4 was added into the reactor. The mixture was stirred for 15 min in the room temperature and then 9.0 g $KMnO_4$ was slowly added into the mixture till the temperature remains under 20°C. Subsequently, temperature was increased to 35°C and stirring was continued for 7 h. Then, 9.0 g $KMnO_4$ was added into the reactor and stirring was continued for additional 12 h at 35°C. The reactor content was diluted by 600 mL deionized water. 30 mL of 30% H_2O_2 was poured into the diluted product to reduce the unreacted $KMnO_4$. After centrifugation and washing the product with hydrochloric acid solution (1/10 in respect to water), wet GO washed three times with distilled water till its pH reaches to about 7. Then, graphite oxide (0.1 mg mL^{-1}) was exfoliated by a probe sonicator at 500 W and 20 kHz (Hielscher Ultrasonics GmbH, UIP500hd, Germany) for 30 min. Finally, dried GO powder was obtained by filtration and vacuum at 65°C.

Reduction of GO by Hydrazine to Yield Reference Graphene Layers

Yellow to brown dispersion of GO (100 mg) in water (100mL) was ultrasonically agitated at 500 W and 20 kHz for 1 h. The dispersion was added into a two-necked balloon which was placed in oil bath at 100°C and equipped with a condenser. Then, hydrazine hydrate (1 mL) was added into the balloon. After 24 h, a black precipitate was obtained after filtration. The filtrate was washed five times by distilled water (100 mL) and ethanol (100 mL). Finally, graphene nanolayers were obtained by vacuum oven at 65°C.

Functionalization of GO by Furfuryl Alcohol Moieties

G-FA was produced by an esterification reaction between the hydroxyl group of furfuryl alcohol and carboxylic acid groups of GO. Nearly 0.2 g GO and 100 mL DMF were poured into a 250-mL flask and objected to stirring by a mechanical device for 15 min. After the homogenization of the suspension, it was further homogenized by exposing to the ultrasound at 500 W

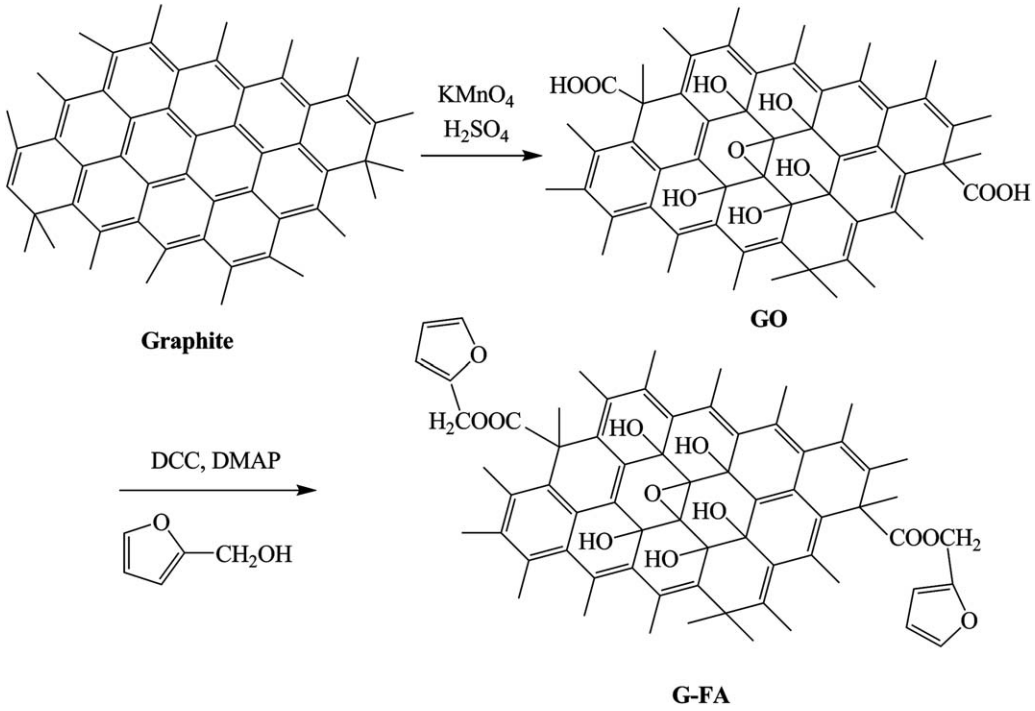

Figure 1. GO modification with furfuryl alcohol.

and 20 kHz and amplitude of 90% for 15 min. Nearly 0.472 mL furfuryl alcohol (5.46 mmol) was added into the reaction medium and stirring was continued for 30 min. Subsequently, a mixture of 4.0 g DCC (20.87 mmol) and 0.3 g DMAP (2.46 mmol) was added dropwise into the flask during 20 min and stirring was continued for 16 hr at room temperature. Finally, after washing the product with DMF for three times, G-FA without free furfuryl alcohol moieties was obtained.

Preparation of Graphene/Novolak Composites

Predetermined values of GO (or G-FA) were added to 11.36 mL furfuryl alcohol and stirring was continued to reach a homogeneous suspension. Subsequently, the product is subjected to a probe sonicator at 500 W and 20 kHz for 20 min. By addition of 0.9 g HMTA and 6.2 g novolak to the system and after agitation for 24 h at the room temperature, the resin compound for molding was obtained. For the molding and curing process, at first, the mold temperature was increased to 90°C and remained in this situation for 9 h. After this stage, the temperate was increased to 135°C by the heating rate of 3.7°C h^{-1}. Subsequently, the mold temperature was increased to 200°C by the heating rate of 12°C h^{-1} and it was held at 200°C for 4 h.

Characterization

Fourier transform infrared (FTIR) spectra were recorded on a Bomem FTIR spectrophotometer (Canada), within a range of 400–4400 cm^{-1} using a resolution of 4 cm^{-1}. An average of 32 scans has been reported for each sample. The cell pathlength was kept constant during all the experiments. The samples were prepared on a KBr pellet in vacuum desiccators under a pressure of 0.01 torr. X-ray diffraction (XRD) spectra were collected on an XRD instrument (Siemens D5000, Germany) with a Cu target ($\lambda = 0.1540$ nm) at room temperature. The system consisted of a rotating anode generator, and operated at 35 kV and a current of 20 mA. The samples were scanned from $2\theta = 2°$ to 10° at the step scan mode, and the diffraction pattern was recorded using a scintillation counter detector. The basal spacing or d_{001}-spacing of the samples was calculated using the Bragg's equation. Raman spectra were collected in the range from 2800 to 1000 cm^{-1} using Bruker Dispersive Raman Spectrometer (Germany) fitted with a 785 nm laser source, a CCD detector, and a confocal depth resolution of 2 μm. The laser beam was focused on the sample using an optical microscope. Thermal gravimetric analyses (TGA) were carried out with a PL thermo-gravimetric analyzer (Polymer Laboratories, TGA 1000, UK). The thermograms were obtained from ambient temperature to 700°C at a heating rate of 10°C min^{-1}. A sample weight of about 10 mg was used for all the measurements, and nitrogen was used as the purging gas at a flow rate of 50 mL min^{-1}; an empty pan was used as the reference. A Vega Tescan SEM analyzer (Czech Republic), was used to evaluate the morphology of the neat and modified graphenes which were gold-coated using a sputtering coater. The specimens were prepared by coating a thin layer on a mica surface using a spin coater (Modern Technology Development Institute, Iran). The transmission electron microscope, Philips EM 208 (The Netherlands), with an accelerating voltage of 120 kV was employed to study the morphology of the nanocomposites; the samples of 70 nm thickness were prepared by Reichert-ultramicrotome.

RESULTS AND DISCUSSION

Graphite was used to prepare GO by an oxidation reaction. Subsequently, it was converted to furfuryl alcohol modified graphene layers by an esterification reaction (Figure 1). GO and G-FA were used to prepare novolak composites with excellent

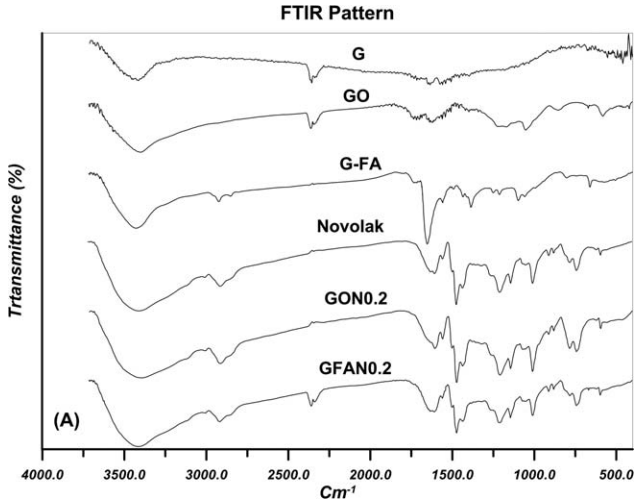

Figure 2. FTIR pattern for graphene, GO, and G-FA, novolak and its composites with two different kinds of modified graphene nanosheets.

thermal characteristics. This is mainly accomplished to evaluate the effect of graphene surface modification on thermal properties and also carbon yield value of the novolak composites. Modification of GO with furfuryl alcohol may result in better dispersion of nanosheets in the novolak matrix because resin curing reaction is carried out in the medium of furfuryl alcohol as the solvent. Graphene layers made from reduction of GO by a hydrazine used as the reference carbon layer in the discussion of the results.

FTIR spectra of graphene, GO, and G-FA in addition to the novolak and its composites are shown in Figure 2. As it is clear, intensified hydroxyl stretching vibration (3398 cm^{-1}), carboxyl stretching vibration (1716 cm^{-1}), and carbon–oxygen vibration (1250 cm^{-1}) can be easily observed after oxidation of graphene sheets. Several characteristic peaks are observed in the FTIR spectra of novolak. The peaks at 2918, 1609, and 1054 cm^{-1} assigned to the CH-stretching vibration of methyl and methylene groups, stretching vibration of nonconjugated carbon–carbon double bonds, and the vibration of C—O band of phenol ether groups respectively indicate that a large number of cross-link structures has formed in the cured novolak resin.[24] OH-stretching vibration is seen in the wave number of 3411 cm^{-1}. Asymmetric CH-bending vibration of methyl and methylene groups results in the peak at 1476 cm^{-1}. The peak at 1438 cm^{-1} comes from the symmetric CH_3-bending vibration of the methyl groups. CH-bending vibration of hexamine results in the wave number of 1213 cm^{-1}. The peaks at 785, 744, and 623 cm^{-1} are related to two or more neighboring hydrogen atoms with different substitutions.[25]

XRD is an effective technique for determination of the extent of graphene dispersion ordered or disordered structure in a polymer composite matrix. Figure 3 displays XRD patterns of the different kinds of graphenes (pristine graphene, GO, and G-FA) and novolak composites with different kinds of graphene respectively. Considering the fact that the mean interlayer space of the (001) plane (d_{001}) can easily be calculated using Bragg's law of diffraction from peak position [eq. (1)], one can evaluate the amount of graphene interlayer expansions by different kinds of modification reactions.

$$d = \lambda/(2\sin\theta) \quad (1)$$

In this equation, d is the interlayer distance, λ is the radiation wavelength of X-ray source that is equal to 1.5406 nm, and θ is the angle of incident radiation.

By oxidation of graphene, the intergallery distance of graphene layers increases from 3.42 to 9.35 nm which corresponds to the decrease of diffraction angle from 26° to 9.45°. The interlayer gallery distance is about 11.04 nm for the G-FA layers ($2\theta = 8°$). This shows that incorporation of oxygen containing functional groups into the interlayer gallery of graphene sheets increases its interlayer distance. In addition, edge functionalization of GO sheets with furfuryl alcohol moieties expands the interlayer gallery. The amorphous peak around 19° is the characteristics of phenolic resins. Considering that there are no other peaks in the XRD graphs of the novolak composites, it can be concluded that all GO and G-FA nanosheets are pushed apart from their stack forms.[26]

Raman spectra for the pristine graphite, graphene, GO, and G-FA are presented in Figure 4. Three peaks at 1343 (D band), 1570 (G band), and 2698 cm^{-1} (2D or G' band) are the characteristics of graphite nanosheets. D peak arises from defects inherent in the graphite and the edge effect of graphite crystallites.[27] G peak is assigned to the first order scattering of the E2g phonon of sp^2 C atoms.[28] The 2D band (G' band) originates from the stacking order of the nanosheets.[29] A perfect graphite crystal does not exhibit the D band. The ratio of the D to G band intensities (I_D/I_G) is reciprocally related to the crystallite size. Therefore, lower amount of defects results in higher crystallite size and also lower value of I_D/I_G. According to the results, peak area of D band is higher for the graphene nanosheets and further increases by oxidation and functionalization of graphene nanosheets. Increasing of I_D/I_G indicates size reduction of graphite sheets by mechanochemical cracking and edge

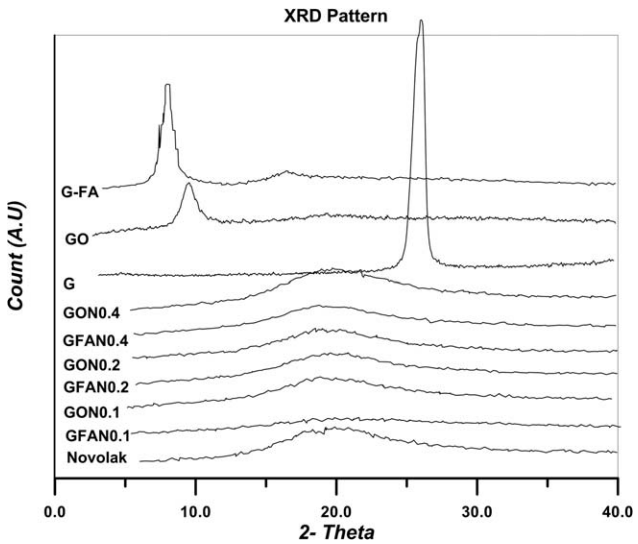

Figure 3. XRD pattern for graphene, GO, G-FA, novolak, and its composites with two different kinds of modified graphene nanosheets.

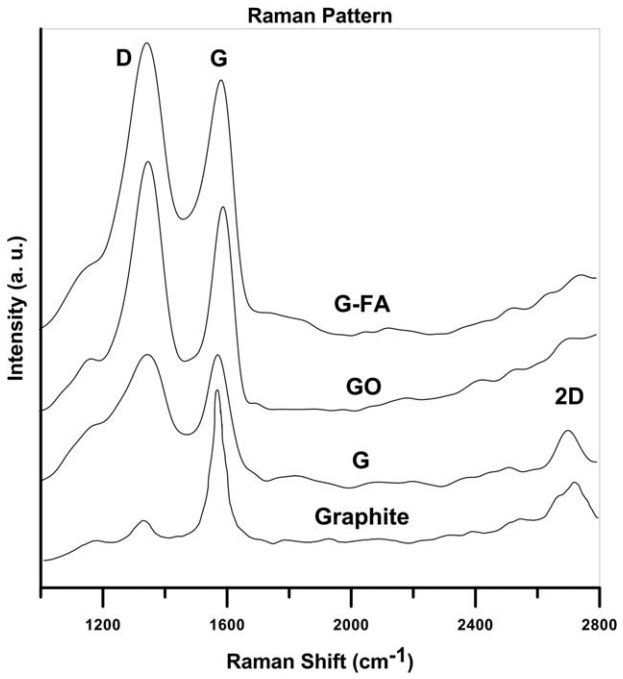

Figure 4. Raman spectra for graphite, graphene, GO, and G-FA.

distortion by functionalization.[29] Thus, graphene nanosheets reduced in size and also wrinkled by the oxidation and functionalization processes. Interaction between the graphene nanosheets increases by oxidation and also functionalization reactions. This results in the formation of relatively bigger grain sizes and tighter aggregates which finally causes sharper *D* and *G* bands.[28] The 2D band is mainly used for the identification of graphene nanosheets since its shape differs from that of the graphite. It is symmetrical for monolayer graphene, but has a shoulder in the case of graphite. Depending on the number of layers, an intermediate shape is obtained for the multilayer graphene nanosheets.[30] Decreasing intensity of this band in the case of GO and G-FA indicates that stacking order is diminished and exfoliated state is achieved.

Thermal stability of the specimens is studied by TGA. Figure 5 illustrates TGA thermograms of weight loss as a function of temperature in the temperature range from ambient temperature to 700°C for the neat and modified graphenes and also novolak and its composites with two different kinds of modified graphene nanosheets. According to the results of graphene nanosheets, pristine graphene reaches to 90.48 wt % char value at 700°C. GO thermogram shows major weight losses between 150 and 220°C corresponding to CO, CO_2, and steam release from the most labile functional groups. Between 230 and 700°C, a slower mass loss is observed which can be attributed to the degradation of more stable oxygen functionalities.[31,32] However, a quite different decomposition pattern was observed after the functionalization of GO with furfuryl alcohol. This can be explained by the loss of most oxygen-containing functional groups during esterification reaction between the carboxylic acid functionalities of GO and furfuryl alcohol in the presence of DCC and DMAP. The 41.49% weight residue in G-FA thermogram up to 700°C is due to the degradation of its modifier and the remained oxygen-containing functional groups. Thermal stabilities of all the composites are higher than the neat novolak. Degradation temperature rises by increasing graphene content. TGA thermograms also shows degradation temperature is lower for composites with lower amounts of graphene and increases by addition of graphene loading. Additionally, char value rises as the amount of graphene increases.

Except for degradation of volatile parts and GO (or G-FA) functionalities at lower temperatures than 350°C, degradation of all the samples takes place in one step and char is left after complete degradation. G-FA loaded composites left more char value than the composites with the same content of GO. This is mainly on account of the fact that the graphene functionalized with furfuryl alcohol is more compatible with the solution of novolak in furfuryl alcohol before the curing reation. Therefore, graphene sheets can be distributed more appropriately during the ultrasonication processes. Additionally, interaction between the furfuryl alcohol moieties of G-FA with the furfuryl alcohol in the novolak matrix network may result in higher carbon yield values. Functionalization of GO may result in a decrease in oxygen-containing functional groups and therefore increase the thermal stability and thermal degradation temperatures. Also, graptitic network can be partly recovered by the functionalization of GO.[33] It can also be understood that increasing graphene content results in an increase of degradation temperature. According to the results, there is an optimum value of GO and G-FA in which the thermal properties reach to its optimum value. By the addition of graphene content, dispersion and delamination of the nanosheets seems to be more complicated. However, the more graphene content added, the higher thermal characteristics should be achieved. Consequently, 0.2 wt % of graphene content is the best value for both types of the composites to reach the higher temperatures for 5 and 10 wt % of matrix degradation. On the other hand, carbon yield value increases sharply by adding only 0.1 wt % of graphene nanosheets. Also, this increment is higher in G-FA loaded composites. About 62% char value at 700°C reveals that this

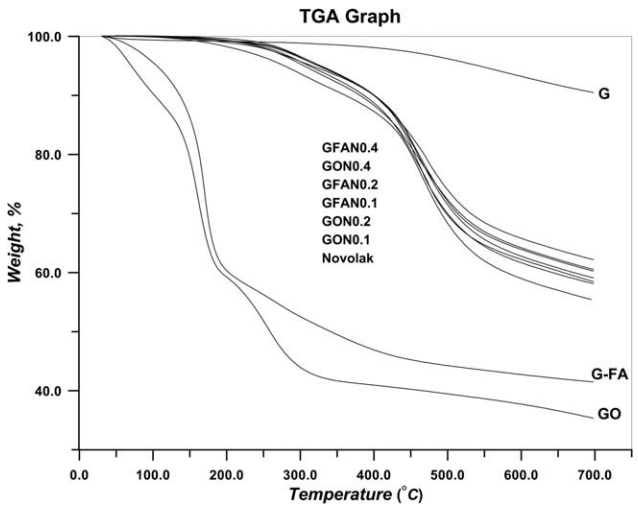

Figure 5. TGA thermograms for graphene, GO, G-FA, novolak, and its composites with two different kinds of modified graphene nanosheets.

Table II. Carbon Yield Values for Different Modified Phenolic Resins

Method	Resin char	Final char	Additive content	Increase (%)	Ref.
Boron-containing (HBp)	64.2	75.4	10%	11.2	34
Boron-containing (HBPB)	63.8	71.3	10%	7.5	8
Boron-containing (HBPB)	63.8	62.1	50%	−1.7	8
Boron-containing (HBPB)	63.8	78.4	80%	14.6	8
Phosphorus-containing (DEPC)	12	39	33%[a]	27	35
Phosphorus-containing (DEPC)	12	43	50%[a]	31	35
Phosphorus-containing (DEPC)	12	47	67%[a]	35	35
MWCNT and Boron-containing	66[b]	68.7	0.25%	2.7	22
MWCNT and Boron-containing	66[b]	70.9	0.5%	4.9	22
MWCNT and Boron-containing	66[b]	72.2	1%	5.2	22
GO-Containing	55.29	60.55	0.4%	5.26	This work
G-FA-Containing	55.29	62.09	0.4%	6.8	This work

[a] Molar ratio.
[b] For boron containing resin.

structure can be maintained after degradation at higher temperatures.

Table II shows carbon yield values for the different phenolic resins. All the data are obtained by the heating rate of 10°C min^{-1} except for MWCNT and boron containing resins which examined at the heating rate of 20°C min^{-1}. Considering the table, a large amount of modifier is needed for increasing the phenolic resins thermal properties. However, MWCNT and graphene sheets even at small amounts can result in the similar findings. Liu and Jing[34] observed that blending of boric acid terminated hyperbranched polyborate (HBp) and phenolic resin can increase the carbon yield value by 11.2% from 64.2 to 75.4 wt % due to the typical mechanisms associated with the boron compounds. They showed that the content of boron was in the range of 0.48–0.80% of the modified phenolic resin. Xu and Jing[8] observed the similar results for the same values of boron compound modifier of hyperbranched polyborate (HBPB). However, increasing the boron modifier compound to the amount of 50% results in decrease of carbon yield value. They attributed this to the decreased curing degree which is induced by the reactions between limited hydroxymethyl groups and the redundant introduced phenol groups of HBPB. In the case of phosphorous containing phenolic resins, the amount of carbon yield increment by adding the diethylphosphoryl chloride (DEPC) as the phosphorous modifier is higher in comparison with the other methods. However, the final value of carbon yield for these materials is low, which is a result of their phenolic resin matrix with low carbon yield value. In the case of additives, very low modifier content can be resulted in the same results obtained from the structural modifiers. Liu and Ye[22] used modified MWCNT as additive to a boron containing phenolic resin. By combining these two methods, they achieved to an increase of carbon yield value by 5.2% with the addition of 1 wt % of MWCNT with respect to the boron containing phenolic resin. Comparison of our product with the reviewed mechanisms shows that by addition of graphene to the phenolic resin, higher carbon yield values can be obtained only at 0.4 wt %. In the case of G-FA added novolak resins, 6.8% addition of char value shows that graphene nanosheets even at lower concentrations acts better than nanotubes for achieving higher carbon yield values. The final carbon yield value of our product could be higher in the case that a phenolic resin with higher value of carbon yield is used in the process. It is an ongoing work at our research group to use a boron containing phenolic resin with the different types of furfuryl alcohol modified graphene nanosheets to examine the final carbon yield value of the resin. We estimate to reach a carbon yield values of more than the reported data for this product.

Also, it is another ongoing work in our group to find that how it could be possible to increase the graphene content in the novolak matrix and observe improvement of thermal characteristics. Thermal characteristics and dispersion ability are improved by using graphene nanosheets with one dimensional functionalization from the edges. Undoubtedly, functionalization of graphene nanosheets from the other dimensions, hydroxide and epoxide functionalities, can result in much more improved properties. Thus, it can be considered as an objective to estimate the effect of each types of functionalization and finally evaluate the results to reach the optimum value of each functionalization to obtain the best thermal characteristics and dispersability of graphene nanosheets in the novolak matrix. Three-dimensional functionalization of graphene nanosheets results in easy dispersion of higher graphene contents and may also increase its degradation temperatures.

Figure 6 displays scanning electron microscopy (SEM) images for graphene, GO, and G-FA respectively. Bare and flat surface of graphene nanosheets are clearly revealed in the Figure 6(a). Although GO sheets are obtained by several sever steps and centrifugation, their well-packed layers can be seen in Figure 6(b). Roughness of the layers is a result of the functional groups of the graphene which can be comprehended by comparison of SEM images. More roughness of graphene sheets is also displayed by SEM image of G-FA. Esterification reaction between hydroxyl groups of furfuryl alcohol and carboxylic acid groups

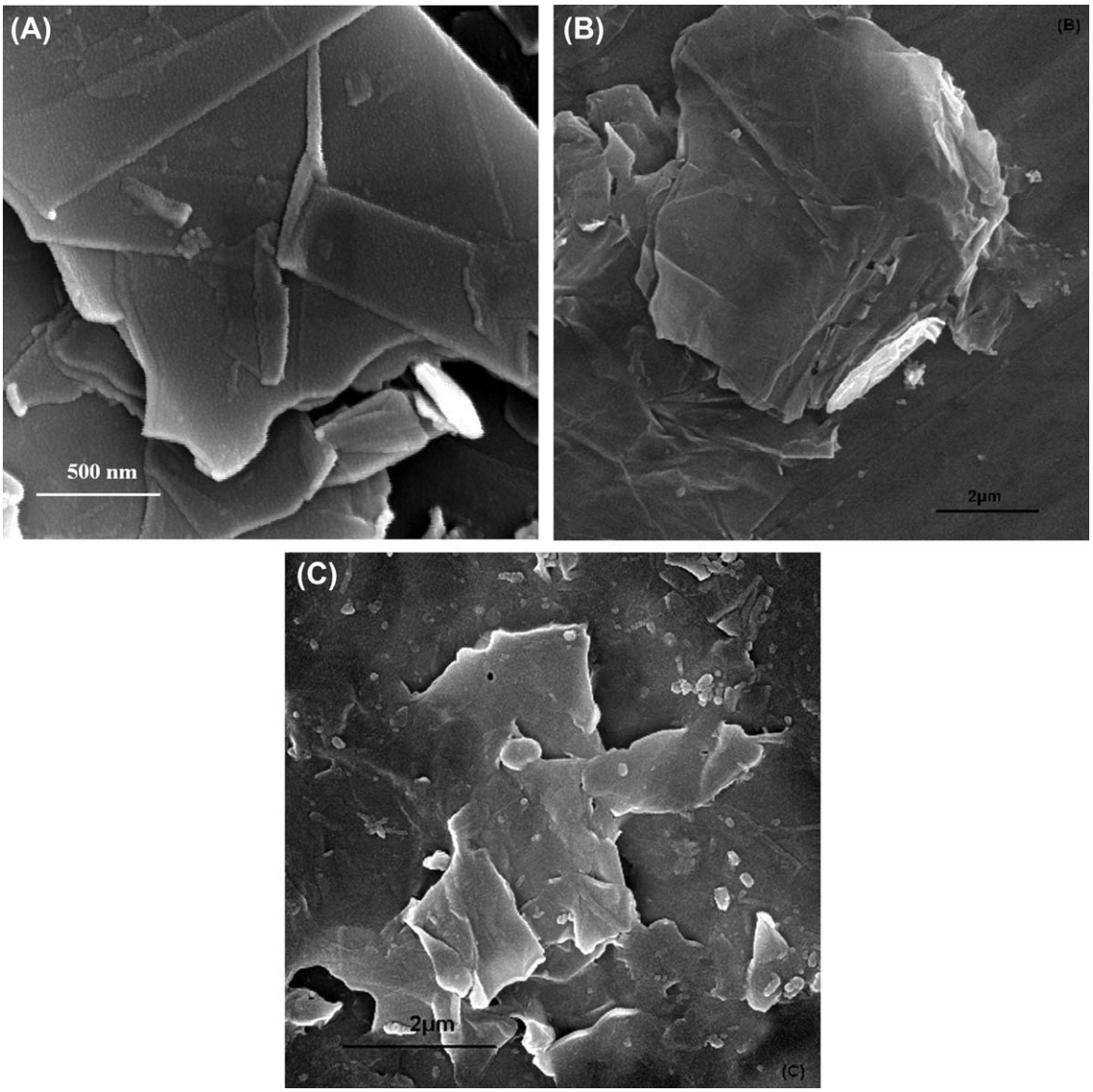

Figure 6. SEM images for (A) graphene, (B) GO, and (C) G-FA.

of GO results in relatively lengthy groups on the GO surfaces. In overall, flat and smooth morphology of graphene nanosheets disturbed in the oxidation and other processes needed for functionalization of graphene nanosheets and therefore wrinkled sheets with curvature are obtained. Also, the surface area of the nanosheets decreases during these processes. The same results were obtained from the Raman spectra by the increasing the value of I_D/I_G ratio indicating the size reduction of graphene nanosheets by edge distortion on account of the functionalization reactions.

Figure 7 represents transmission electron microscopy (TEM) image of novolak/G-FA composite with 0.2 wt % of nanosheet content and clearly demonstrates the presence of G-FA in the novolak matrix. Relatively dark and light areas display the rough nanosheet of G-FA and novolak matrix respectively.

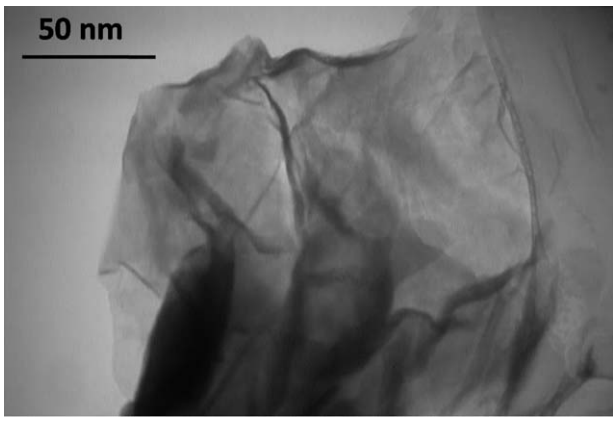

Figure 7. TEM micrograph of GFAN0.2.

Wrinkled nanosheets with high surface area are seen in the image.

CONCLUSIONS

GO and furfuryl alcohol modified graphene (G-FA) were used to prepare graphene/novolak composites and also study of the effect of filler compatibilization on its properties. Graphene sheets are dispersed uniquely in the matrix of the composites with lower graphene content. Modification of graphene sheets by furfuryl alcohol results in better dispersions. Graphene nanosheets reduced in size, wrinkled, and also their stacking order is diminished by the oxidation and functionalization processes. Thermal stability of the composites increases by adding graphene nanosheets. Composites with G-FA show higher char value after degradation at high temperatures in comparison with the GO-filled composites. Results show that 0.2 wt % of graphene content is the best value to reach high level of dispersion, higher carbon yield value, and higher thermal degradation temperature. A 6.8% addition of carbon yield value for the G-FA added novalak resin makes graphenes more preferable than nanotubes to reach high thermal characteristics even at lower concentrations. Three-dimentional functionalization of graphene nanosheets can not only result in easy dispersion of higher graphene contents in the novolak matrix, but also increase its degradation temperatures. Wrinkling and size reduction of the graphene nanosheets after oxidation and modification and also the structure of G-FA nanosheets in the matrix of novolak are evaluated by electron microscopy.

REFERENCES

1. Yamashita, Y.; Ouchi, K. *Carbon* **1979**, *17*, 365.
2. Sonobe, N.; Kyotani, T.; Tomita, A. *Carbon* **1990**, *28*, 483.
3. Wewerka, E. M.; Walters, K. L.; Moore, R. H. *Carbon* **1969**, *7*, 129.
4. Manocha, L. M. *Carbon* **1994**, *32*, 213.
5. Ma, C. C. M.; Lee, C. T.; Wu, H. D. *J. Appl. Polym. Sci.* **1998**, *69*, 1129.
6. Gao, J. G.; Liu, Y. F.; Yang, L. T. *Polym. Degrad. Stab.* **1999**, *63*, 19.
7. Ogoshi, T.; Saito, T.; Yamagishi, T.; Nakamoto, Y. *Polymer* **2009**, *47*, 117.
8. Xu, P.; Jing, X. *Polym. Adv. Technol.* **2011**, *22*, 2592.
9. Roghani-Mamaqani, H.; Haddadi-Asl, V.; Salami-Kalajahi, M. *Polym. Rev.* **2012**, *52*, 142.
10. Saini, P.; Choudhary, V.; Singh, B. P; Mathur, R. B.; Dhawan, S. K. *Mater. Chem. Phys.* **2009**, *113*, 919.
11. Saini, P.; Choudhary, V.; Singh, B. P.; Mathur, R. B.; Dhawan, S. K. *Synth. Met.* **2011**, *161*, 1522.
12. Saini, P.; Choudhary, V. J. *Nanopart. Res.* **2013**, *15*, 1415.
13. Singh, B. P.; Saini, P.; Gupta, T.; Garg, P.; Kumar, G.; Pande, I.; et al. *J. Nanopart Res.* **2011**, *13*, 7065.
14. Qi, X. Y.; Yan, D.; Jiang, Z.; Cao, Y. K.; Yu, Z. Z.; Yavari, F.; Koratkar, N. *ACS Appl. Mater. Interfaces* **2011**, *3*, 3130.
15. Saini, P.; Choudhary, V.; Dhawan, S. K. *Polym. Adv. Technol.* **2009**, *20*, 355.
16. Saini, P.; Choudhary, V.; Sood, K. N.; Dhawan, S. K. *J. Appl. Polym. Sci.* **2009**, *113*, 3146.
17. Banerjee, S.; Hemraj-Benny, T.; Wong, S. S. *Adv. Mater.* **2005**, *17*, 17.
18. Kim, H.; Abdala, A. A.; Macosko, C. W. *Macromolecules* **2010**, *43*, 6515.
19. Men, X. H.; Zhang, Z. Z.; Song, H. J.; Wang, K.; Jiang, W. *Compos. Sci. Technol.* **2008**, *68*, 1042.
20. Yeh, M. K.; Tai, N. H.; Liu, J. H. *Carbon* **2006**, *44*, 1.
21. Choi, W. S.; Shanmugharaj, A. M.; Ryu, S. H. *Thermochim. Acta* **2010**, *506*, 77.
22. Liu, L.; Ye, Z. *Polym. Degrad. Stab.* **2009**, *94*, 1972.
23. Cui, J.; Yan, Y.; Liu, J.; Wu, Q. *Polym. J.* **2008**, *40*, 1067.
24. Trick, K. A.; Saliba, T. E. *Carbon* **1995**, *33*, 1509.
25. Theodoropoulou, S.; Papadimitriou, D.; Zoumpoulakis, L.; Simitzis, J. *Anal. Bioanal. Chem.* **2004**, *379*, 788.
26. Dante, R. C.; Santamaria, D. A.; Gil, J. M. *J. Appl. Polym. Sci.* **2009**, *114*, 4059.
27. Fang, M.; Wang, K.; Lu, H.; Yang, Y.; Nutt, S. *J. Mater. Chem.* **2010**, *20*, 1982.
28. Hu, H.; Wang, X.; Wang, J.; Wan, L.; Liu, F.; Zheng, H. *Chem. Phys. Lett.* **2010**, *484*, 247.
29. Jeon, I. Y.; Choi, H. J.; Jung, S. M.; Seo, J. M.; Kim, M. J.; Dai, L. *J. Am. Chem. Soc.* **2013**, *135*, 1386.
30. Sanna, R.; Sanna, D.; Alzari, V.; Nuvoli, D.; Scognamillo, S.; Piccinini, M. *J. Polym. Sci. A Polym. Chem.* **2012**, *50*, 4110.
31. Stankovich, S.; Dikin, D. A.; Piner, R. D.; Kohlhaas, K. A.; Kleinhammes, A.; Jia, Y. *Carbon* **2007**, *45*, 1558.
32. Shen, J.; Hu, Y.; Shi, M.; Lu, X.; Qin, C.; Li, C. *Chem. Mater.* **2009**, *21*, 3514.
33. Roghani-Mamaqani, H.; Haddadi-Asl, V. *Polym. Compos.* **2013**.
34. Liu, Y.; Jing, X. *Carbon* **2007**, *45*, 1965.
35. Hsiue, G. H.; Shiao, S. J.; Wei, H. F.; Kuo, W. J.; Sha, Y. A. *J. Appl. Polym. Sci.* **2001**, *79*, 342.